XI. Materials

ENGINEERING MECHANICS DIVISION

A. Spacecraft Adhesives for Long Life and Extreme Environment, *W. D. Roper*

1. Introduction

The present state-of-the-art of high performance adhesives is being reviewed to establish those new adhesive materials which show promise as spacecraft adhesives for use in future planetary missions. In these future missions it is anticipated that structural adhesives will be required to function for extensive periods in environmental extremes ranging from above 500°F to −375°F. The performance requirements on adhesive materials will, therefore, be quite high and will go beyond what has thus far been required of spacecraft adhesives.

The studies performed have been divided into two phases. The first phase consisted of a state-of-the-art literature review in order to determine all the promising new materials which could be considered for future spacecraft use. This review was completed and reported previously (SPS 37-63, Vol. III, pp. 128–133). The second phase of the work unit consisted of a limited laboratory evaluation of the candidate adhesives which were selected from the Phase 1 review. The results of some of this laboratory evaluation are now being reported.

The polymeric materials that were selected for laboratory evaluation as adhesives were the polyimide (PI), polybenzimidazole (PBI), and the polyquinoxaline (PQ) polymers. As adhesives these materials were evaluated for thermal shock resistance and for long-term aging at both elevated and cryogenic temperatures. The thermal shock testing was recently completed and the long-term aging tests are currently in process.

2. Adhesive Thermal Shock Evaluation

a. Test specimen preparation. The two commercially available adhesives selected were the polyimide adhesive, FM-34 (American Cyanamid Co., Bloomingdale Dept.) and the polybenzimidazole, Imidite 850 (Whittaker Corp., Narmco Materials Division). Both of these adhesives were supplied as films supported by fiberglass carriers. The polyquinoxaline material was purchased as a resin solution (Whittaker Corp., Research and Development Division). This material required further processing in the laboratory in order to prepare it as a fiberglass-supported adhesive film. For comparison purposes, a typical epoxy paste-type adhesive, Epon 913 (Shell Chemical Co.), was also selected for testing along with the newer materials. This particular epoxy adhesive was selected because it had been used frequently in the past in spacecraft fabrication.

The selected adhesives were prepared into standard lap shear specimens and were tested according to the

ASTM D1002 (American Society for Testing and Materials) test procedure. The testing was performed to evaluate the metal-to-metal bond strength of each and the effect of high thermal shock on this bond strength. Since the cure temperatures and the anticipated service temperatures of the adhesives were well above 500°F, high temperature adherends were necessary. Consequently the adhesives were evaluated for the metal-to-metal bonding of titanium. The lap shear specimens were prepared using titanium (6Al-4V) adherends. In the case of the epoxy adhesive, which was used only for comparison purposes, a typical spacecraft aluminum alloy (6061-T6) was used.

b. Thermal shock cycling. The thermal shock testing performed in these studies was designed to simulate a condition typical of what might be expected in a near-sun type of mission (Mercury or Venus flyby). In this case, rapid structural temperature changes between 400°F and −100°F may be typical during a midcourse maneuver (Ref. 1). The thermal cycling used in these studies was therefore as shown in Fig. 1. In this exposure, specimens of each adhesive were given two thermal cycles between the 400°F and −100°F temperature extremes. Some *in situ* adhesion testing of the materials was also performed at the −100°F extreme as well as before and after the cycling. As seen from Fig. 1, the thermal shock rates experienced by the adhesives ranged between 25 to 55°F/min. A thermal shock of this order could be considered typical of a Venus-type mission (Ref. 1).

The procedure used in the cycling was as follows:

(1) Lap shear test specimens of each adhesive were tested at room temperature in order to establish the room temperature strength of each of the adhesives. The specimens were tested according to the ASTM D1002 test method.

(2) Approximately nine specimens of each adhesive were then placed in a preheated 400 ±10°F oven. The warm-up of the specimens was monitored by a temperature recorder using thermocouples mounted on the specimens.

(3) When the specimens reached 400 ±10°F, they were allowed to soak at that temperature for 10–15 min. They were then removed and quickly placed inside a prechilled −100 ±10°F chamber. The specimen cool-down was again continuously recorded during the cooling process.

(4) After the specimens reached −100 ±10°F, specimens of each material were pulled *in situ* on a tensile testing machine according to the ASTM D1002 test method.

(5) Following the −100°F testing, the remaining specimens were again rapidly heated to 400 ±10°F in the preheated oven. The temperature of the specimens was again continuously recorded.

(6) After soaking at 400 ±10°F for 10–15 min, the specimens were then removed from the oven and again rapidly chilled in the −100 ±10°F chamber. Specimens of each material were then tested *in situ* at the −100°F temperature.

(7) Following the second chilling and *in situ* testing, the last remaining specimens were then warmed to room temperature and tested at this temperature.

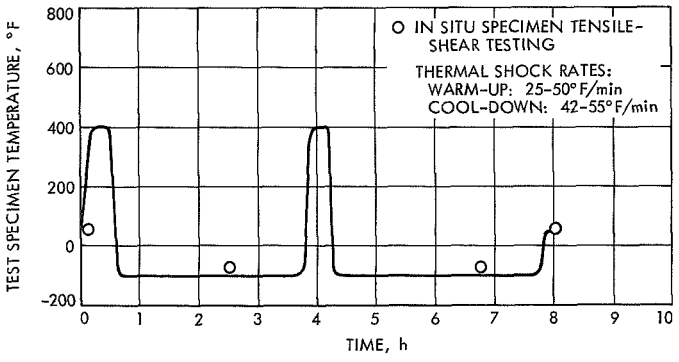

Fig. 1. Adhesive thermal shock testing

In addition to the preceding specimen testing, an attempt was also made to evaluate the creep resistance of the FM-34 and the PQ adhesives. To accomplish this, one creep test specimen of each adhesive was prepared according to the ASTM D2294 test procedure. The specimens were mounted in creep test fixtures and were each placed under a 750-psi tensile load. The specimens were then subjected to the same thermal shock as given to the lap shear specimens. The creep test specimens were observed for evidence of creep or bond failure during the exposure to the thermal shock.

3. Results and Discussion

The lap shear adhesion data obtained on each adhesive during the thermal shock testing are shown in Table 1. The data include lap shear strength of the adhesives at room temperature prior to cycling, at −100°F during cycling, and again at room temperature at the end of the two thermal cycles. These data permit some evaluation of the overall effect of the cycling as well as some evaluation of the adhesives at the lower temperature extreme. Resources precluded testing at the 400°F temperature extreme. Table 1 also shows the results obtained with the creep test specimens which were subjected to the same thermal cycling as the lap shear specimens.

Table 1. Thermal shock test data

Adhesive	Adherend	Tensile-shear strength, psi				Creep, mils
		Cycle 1		Cycle 2		
		75°F	−100°F	−100°F	75°F	
Imidite 850 (PBI)	Titanium 6Al-4V	1630	1160	1040	1100	Not tested
		1350	1130	1250	1100	
		1440	1380		1360	
		1540				
		Av 1490	1160	1150	1190	
FM-34 (PI)	Titanium 6Al-4V	2560	2720	2150	1850	0
		1620	2450	2640	1610[a]	
		2780	2780	3160	1420[a]	
		Av 2320	2650	2650		
Polyquinoxaline (PQ)	Titanium 6Al-4V	1690	1880	1220	1790	0
		2110	1430	1520	2310	
		1260				
		Av 1690	1660	1370	2050	
Epon 913 (epoxy)	Aluminum 6061-T6	3090	1720	1540	3920	Not tested
		4170	2060	1930	3860	
		4360	1830		3790	
			Av 3870	1870	1740	3860

[a]Defective specimen.

Of the newer adhesives tested, the polyimide, FM-34, gave the highest bond strength at room temperature. The polyquinoxaline was only slightly higher in strength than the polybenzimidazole, Imidite 850. The epoxy adhesive, Epon 913, had the greatest strength of all. However, it should be noted that the epoxy bonding was on aluminum, whereas the new high temperature adhesives were on titanium. Bond strengths are generally significantly lower on titanium substrates as compared to aluminum or steel alloys.

The data obtained on the polybenzimidazole adhesive (Imidite 850) were particularly interesting. The two thermal cycles resulted in an overall bond strength loss of approximately 20%. The data taken during the cycling at −100°F indicates that this loss occurred during the first cycle. After the first cycle the bond strength remained essentially constant at the 20% lower level. Statistical treatment of the data indicated that this strength loss was real to a better than 95% confidence level. The strength loss after the first cycle was apparently nonrecoverable when rewarmed to room temperature. No difference in the mode of specimen failure could be observed during the pulling of the specimens. The specimen failure was in all instances 90% or more cohesive (failure within the adhesive).

The cause of the strength loss can only be speculated. It is suspected that bond damage occurred during the chilling phase of the first cycle due to thermal contraction effects. As noted earlier, in the adhesives review, some polybenzimidazoles may exhibit more than one glass transition temperature (T_g). One PBI polymer has been found to have three, one of which is in the region of −94°F (Ref. 2). The PBI adhesive evaluated in these studies may also exhibit some low T_g value. If this is the case, this may account for the apparent loss in bond strength which occurred on chilling the adhesive to −100°F. If the material had passed through a low temperature T_g, then some bond damage may have occurred due to resultant physical property changes of the adhesive. Another cause may have simply been that the PBI structure was too rigid to adequately respond to the rapid thermal shock imposed. A complete investigation of the cause of the PBI strength loss during thermal cycling was beyond the scope of these studies.

The data obtained on the polyimide adhesive, FM-34, showed that the adhesive tensile-shear strength at room temperature and −100°F were essentially the same. No significant embrittlement of the adhesive, therefore, occurred at the low temperature. The mode of specimen failure with all the specimens was 90% or more cohesive. No creep was exhibited by the creep test specimens which were also thermal cycled with a 750-psi tensile load. Investigation of the two low tensile-shear values (1610 and 1420 psi) in the final room temperature tests revealed that these specimens were defective due to panel misalignment during bonding. These values were not, therefore, averaged as they were not representative of good specimens. Since all the other specimens tested throughout the cycling showed essentially the same strength, it was apparent that the thermal cycling had not affected the adhesive. This observation was also in line with the fact that all reported T_g values for polyimides are in excess of 500°F. Therefore, it did not seem likely that the chilling of the polyimide adhesive to −100°F should affect the adhesive performance due to passage through a T_g region.

The polyquinoxaline adhesive also did not seem affected by the thermal shock cycling. Its low temperature strength was essentially the same as that at room temperature. No creep was obtained with the creep test specimens which were thermal cycled with a 750-psi tensile load. The specimen failures during testing were approximately 40% cohesive. This indicated that the bond strength obtained was not maximized. Inexperience in the processing and formulation of the resin into an adhesive material was very likely a cause. No attempt was made to optimize the processing of this material into high strength bonds. It was conceivable that higher bond strengths can be

achieved with further development of this material as an adhesive.

The epoxy adhesive, Epon 913, was given the thermal shock cycling to compare its performance with that of the newer adhesive materials. As can be seen from the test data, the adhesive has high room temperature strength but it experiences considerable embrittlement at the lower (−100°F) temperature. This is not too surprising as epoxy adhesives are generally reported to have brittle points in the region of −70°F. The mode of failure for the specimens pulled at room temperature was almost 100% cohesive. The mode was significantly different with the −100°F specimens. At this low temperature, the specimens pulled only 30–40% cohesively. Embrittlement of the adhesive at the low temperature was, therefore, very evident. However, this embrittlement was reversible as the adhesive regained its room temperature strength after the cycling. The specimens pulled at room temperature after the two thermal cycles also pulled about 100% cohesively. The thermal cycling, therefore, did not apparently damage the adhesive.

4. Conclusions

The thermal shock testing of the adhesives provided an effective screening for the determination of suitable spacecraft adhesives. On the basis of the shock testing, the order of decreasing preference of the adhesives for future spacecraft application was: polyimide, polyquinoxaline, and polybenzimidazole. The shock testing showed that the polyimide was by far the better adhesive. Its tensile-shear strength remained relatively unchanged within the range of 75 to −100°F. It was also unaffected by the high rates of thermal shock to which it was subjected. The polyimide was also the most attractive on the basis of handling ease and required only moderately high cure temperatures and pressures. The polyimide could, therefore, be considered in structural bonding applications in future spacecraft where high thermal shock will be encountered.

The polyquinoxaline withstood the high thermal shock exposure. However, its bond strength on titanium was not particularly impressive. The PQ requires development into a fully compounded adhesive. Optimization of its formulation may then result in improved bond strengths. At present, it is the most difficult to process into adhesive bonds as it requires carrier prepregging and lengthy high temperature cures. Part of this handling could be reduced if the material ultimately achieves commercial availability as a fiberglass-supported film. The polybenzimidazole was not particularly attractive as a potential spacecraft adhesive. Its bond strength on titanium was found to be quite low and would not be sufficient for structural bonding. At the same time the material appeared to be affected by the thermal shock used in these studies. On the basis of the testing, the PBI showed no particular advantage over either the polyimide or polyquinoxaline adhesives.

As stated earlier, these same adhesives will be evaluated for their long-term aging at elevated and at cryogenic temperatures. Consequently, they are currently being exposed to 500°F at 10^{-6} torr. It is planned that this exposure will be continued for a period of 5000 h. This testing will provide further characterization of these materials. Long-term aging tests at cryogenic (−375°F) temperature levels are planned for the future.

References

1. Ragsdale, G. C., and Mesnard, D. C., *Mariner Venus 67 Spacecraft Environmental Test Results*, Technical Report 32-1249. Jet Propulsion Laboratory, Pasadena, Calif., June 15, 1968.
2. Gillham, J. K., "Thermomechanical Behavior of a Polybenzimidazole System by Torsional Braid Analysis," *Am. Chem. Soc. Polymer Preprint*, Vol. 7, pp. 513–519, 1966.

B. Cracking of Filter Layers in a High Performance Solar Cell Filter, *W. Jaworski*

1. Introduction

For spacecraft flights in the vicinity of Mercury or even closer to the sun, high performance filter covers are required to protect solar cells from exceeding the allowable temperature. Temperatures substantially higher than 140°C cause a steep degradation of solar cell power conversion; they also may induce some disintegration of cell interconnecting structure. The purpose of the filter is, therefore, to reduce as much as possible the solar energy outside of the visible (power convertible) wavelengths region (mostly infrared), and, in this way, keep the cell temperature within desired limits.

A filter of the described characteristic is generally an interference-type filter, normally of a complex design. It contains several stacks of filter layers, grouped to reflect certain predetermined bandwidths of solar irradiation. These layers are vacuum-deposited on a fused silica glass to form a filter cover. Each stack may consist of a considerable number of such layers that are composed of different materials. Thus, the compatibility of multilayer interference filters with the space environment (particularly thermal) becomes one of the major considerations.

In the Advanced Research and Development program related to solar arrays suitable for swingby Venus–Mercury missions, a number of solar cell–filter combinations have been experimentally investigated. Among them, a modified 4026 filter cover[1] mounted on a 2-Ω-cm solar cell was found to be the most promising. This filter has three multilayer stacks superimposed on one another, each containing a number of different layer materials.

During the exploratory 500-h test for ultraviolet and particle irradiation effects, several modified 4026 filter covers and solar cell–filter combinations were subjected to vacuum–temperature exposure. First, vacuum of approximately 5×10^{-7} torr was applied to the samples; then the temperature of the samples was raised from room temperature (approximately 15 to 20°C) to about 140°C. As a result, mosaic-pattern cracks appeared. These cracks were more severe in the cell–filter assemblies than in the filter covers alone.

The purpose of this article is to discuss a probable cause of the damage and possible environmental incompatibility of the modified 4026 interference filter.

[1]Optical Coating Laboratory, Inc., designation.

2. Description and Examination of the Damage

The irradiation test setup in the test chamber consisted of eighteen samples; three samples were modified 4026 filter covers, three modified 4026 filter covers on 2-Ω-cm cells, and the remainder was an assortment of other filter covers and solar cell–filter combinations. As stated above, all of these samples were subjected to a vacuum and elevated temperature to establish the test conditions for starting the 500-h irradiation exposure.

Shortly before exposure to the irradiation fluxes, it was observed that the solar cell assemblies with modified 4026 filter exhibited local cracks (seen through the chamber window) which, by appearance, remained unaltered until the end of 500 h of testing. The actual in-depth location of the cracks within the cell–filter assembly could not be determined by visual inspection after the test, and further investigation was necessary to identify the surface of the cracks and their penetration. Figures 1a and b show the cell–filter assembly before and after the cracks appeared.

To determine the position of the crack surface in the solar cell–filter assembly (see Fig. 2), a Brinkmann vernier microscope was used. By precision focusing the following distances were measured:

Glass top to apparent crack surface	350 μm
Glass top to cell surface	589 μm

Assuming an average index of refraction for the fused silica glass (wavelength between 0.4 and 0.7 μm) to be 1.46 (see Ref. 1), the real distance of crack surface from the top of the glass becomes $y = 350 \times 1.46 = 511$ μm (~0.0201 in.). This is exactly the thickness of the 20-mil glass used (considering tolerance). Thus, it was established that the surface of the crack was adjacent to the glass–filter interface. The difference of $589 - 511 = 78$ μm was the thickness of filter layer stacks and the adhesive (normally about 20 to 30 μm).[2]

To establish crack penetration, an attempt was made to separate the filter cover from the cell by using an adhesive softener. This turned out to be a successful operation, and the separation was accomplished without disturbing the filter layers. Figure 1c shows the underside of the filter cover after separation. It is clearly seen that the crack pattern is identical with that shown in Fig. 1b.

[2]Distance from the glass top to the cell surface was measured directly, since the cell's edge projected outside the glass (see Fig. 2).

(a) CELL-FILTER BEFORE EXPOSURE (20×)

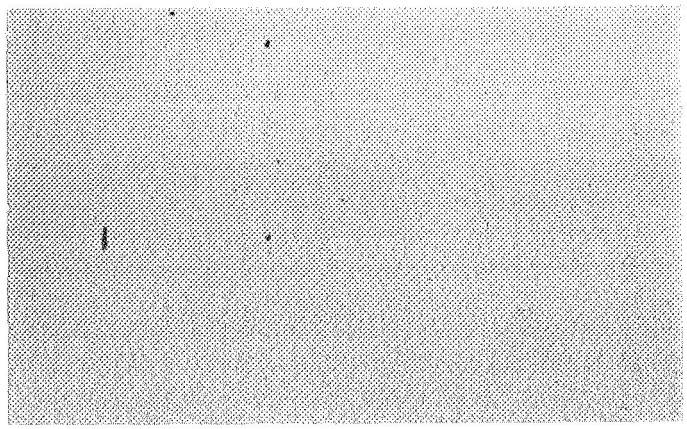

(b) CELL-FILTER AFTER EXPOSURE (20×)

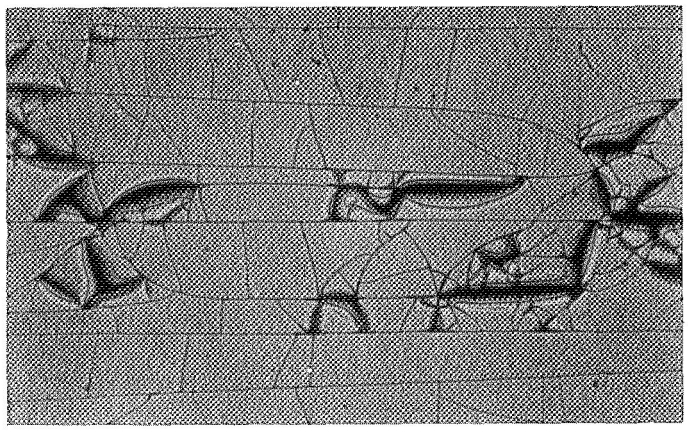

(c) UNDERSIDE OF FILTER COVER AFTER SEPARATION (20×)

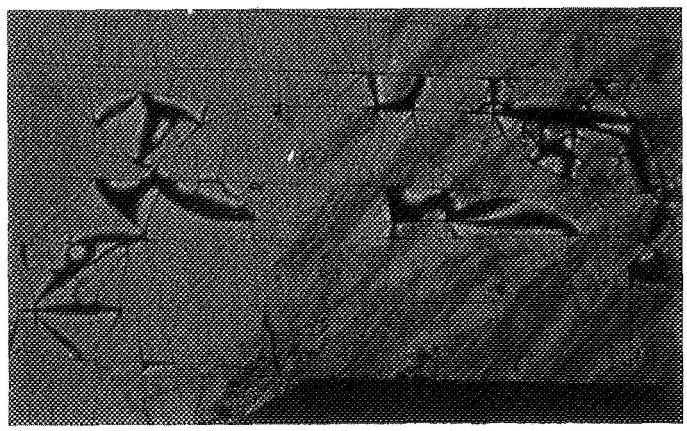

Fig. 1. Cracking of filter layers in a cell–filter assembly during vacuum–temperature exposure

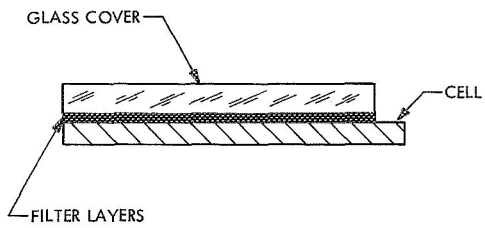

Fig. 2. Section through solar cell–filter assembly

(a) FILTER LAYERS PARTIALLY REMOVED (20×)

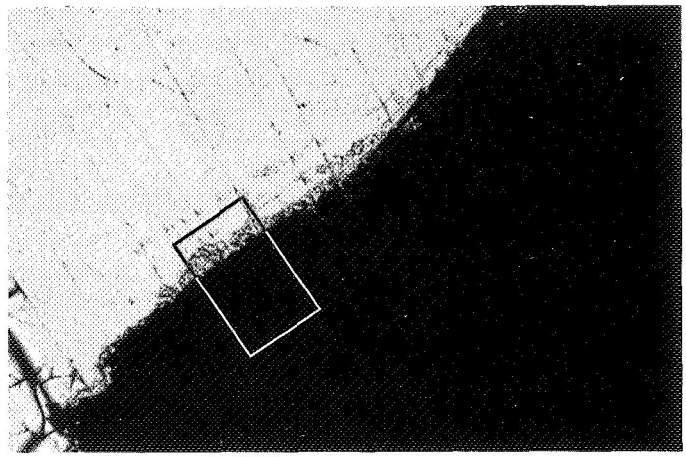

(b) ENLARGEMENT OF BOXED AREA IN (a) (100×)

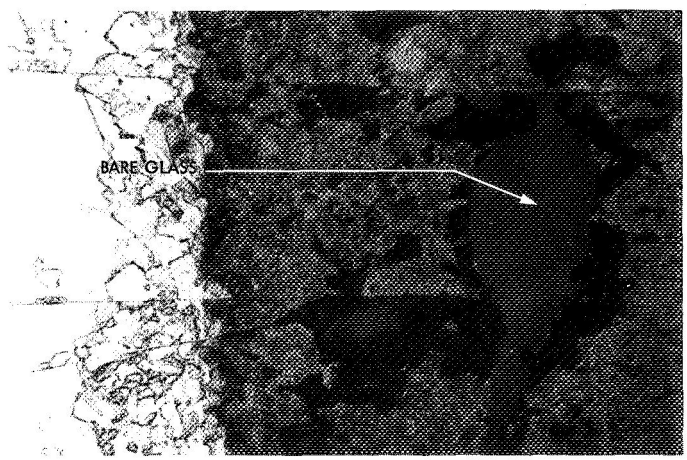

Fig. 3. Partial removal of filter layers to expose the bare glass

By visual inspection of the underside of the filter cover, it was ascertained that all of the filter stacks cracked through along the pattern lines. However, it was still of some interest to know whether the surface of the glass in contact with the filter was in any way affected. To determine this, the filter layers were partially removed from the glass by scraping. Figure 3a shows a portion of the underside of the filter cover (shown in Fig. 1c) over which filter layers were partially scraped (very dark part). In this scraped dark area there are several spots in which the filter layers were completely removed from the glass,

some of them extending across the crack pattern lines seen in the unscraped part (light portion of the picture).

Figure 3b shows a magnified view of the boxed area indicated on Fig. 3a which shows one of the bare glass spots (uniform dark grey pear-shaped area on the right side of the picture). It is seen that where this spot extends across the filter crack line, the line does not extend through the bare glass, signifying no cracking in the glass.

Similar filter cracking was also discovered in the samples representing modified 4026 filter cover alone. The crack lines, however, were less pronounced and probably caused by lower stresses than those present in a cell–filter assembly. Figure 4 shows these cracks in a filter cover sample.

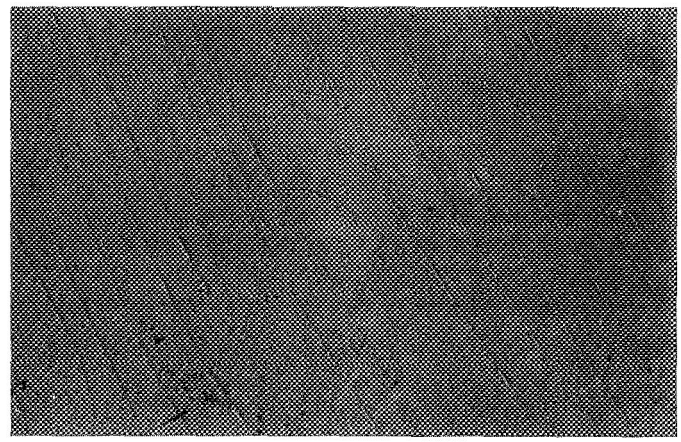

Fig. 4. Cracking of filter layers in a filter cover during vacuum–temperature exposure (20×)

3. Evaluation and Discussion

The presented cracking phenomena of modified 4026 filter layers under vacuum–temperature exposure reveal an undesirable design characteristic. Although the cracks did not grow as exposure continued, there is no guarantee that when thermal shocks, such as those occurring during planet occultation or spacecraft maneuvers, are applied, extensive damage to a solar array would not occur. The cracking was probably a result of initial stresses set in during manufacture of this very complex filter, aggravated by an exposure to substantial temperature change.

On the plus side of this evaluation is some evidence that the cracking of filter layers does not always take place. Two subsequent simulation tests, made in different facilities, have not produced any cracking in modified 4026 cell–filter assemblies. This would imply that initial manufacturing stresses or some imperfections in vacuum deposition of filter layers could be primarily responsible for the cracking. However, filter layers, cover glass, and solar cell are all made of different materials or groups of materials; thus the compatibility problem appears to be rather complex.

This filter has very desirable optical characteristics which do not change significantly when cracking, such as described here, does take place. Therefore, the stability of the extent of cracking would probably be of more interest to solar array designers than a complete prevention of cracking. In any event, more research is needed to clearly pinpoint the cause of cracking, and to find a solution to this problem.

Reference

1. Malitson, T. H., "Interspecimen Comparison of the Refractive Index of Fused Silica," *J. Opt. Soc. Am.*, Vol. 55, No. 10, pp. 1205–1209, Oct. 1965.

C. Development of a Conical–Gregorian High-Gain Antenna, *J. G. Fisher*

1. Introduction

In SPS 37-63, Vol. III, pp. 124–128, initial efforts in the construction of a furlable conical–Gregorian high-gain antenna are described. The first furlable model used 0.005-in.-thick hard-rolled stainless steel as the reflective membrane, which must bend to a conical surface in the furled state (see Fig. 7 on p. 127 of SPS 37-63, Vol. III). As was noted in the referenced SPS, the 0.005-in.-thick reflective membrane would not retain the required conical surface when the antenna was rotated to an axis-horizontal position for RF testing in a one-*g* field. Several schemes for supporting the membrane were considered. In general, these employed circumferential stiffening members which would deploy to lie perpendicular to the reflective surface when the antenna was opened. Practical fabrication difficulties left each of these schemes open to question. It was decided to try using a thicker, and thus stiffer, material for the membrane itself, and thus avoid the use of extra members. The problems associated with the design, construction, and testing of an antenna built in this way are discussed.

2. Design Considerations

To make the reflective surface essentially self-supporting, it appeared advisable to use as thick a material as would accept the bending required for furling without exceeding the elastic limit of the alloy chosen. A low modulus of elasticity/yield strength ratio would thus be desirable, with low density a secondary characteristic. A sample of 0.020-in.-thick 2024-T3 aluminum alloy was bent to the radius observed in the 0.005-in. stainless steel model, and it returned to flat on release. It was decided to use this material for the test.

3. Construction Details

The required eight panels were cut using the same template used for the stainless steel model. However, at the request of the Telecommunications Division, extra material was left at the inner edges to pick up RF spillover which had been observed during testing of the earlier configuration. As in the later-model stainless membrane antenna, the hinge pins were located in the plane of the reflective surface, to avoid opening at the ribs. Also, in an effort to avoid bending loads across the hinge–ribs, and thus retain a more precise surface, the panels were precurved to the deployed conical shape. Final assembly was made on the previously used plaster mandrel using epoxy adhesive (Scotchweld 2216).

4. Furling Test Results

The first furling test was made manually, since a mechanism was not available. The antenna, with its subdish and supports in position, was oriented face up, and the ribs raised simultaneously. About half-way to the furled position, the epoxy adhesive bond between the membrane panels and the hinge–rib flanges began to break loose, especially at the inside ends of the panels. The test was stopped, and the antenna redeployed. Examination of the structure showed no plastic deformation, and it was concluded that the thicker aluminum membrane was merely introducing more stress into the bond joints than the adhesive could hold. The panels were therefore removed from the hub and rivets used to join the membranes to the hinge flanges. During the initial furling, it had been noticed that the ribs tended to flex in the direction of furling, as though being overpowered by the aluminum membrane. It was decided to use the same rivets to fasten angles to the hinge flanges and thus stiffen them against this bending. Because the hinges had to close in the furled position, only small angles, about a quarter inch high, could be used, but by offsetting them slightly, they could be made to nest in the furled position.

With these modifications, the furling test was resumed. This time it was found that considerable force was required to close the antenna, especially as the hinge–ribs were pushed between the subdish supports. The aluminum panels did not curve in the same way as the stainless steel ones. The latter had bent easily to a horseshoe shape, and had slid without difficulty between the subdish supports. The thicker aluminum curved in a more circular bend, and could be pushed between the legs only with considerable force. Also, in the stainless steel model, the sharpest curve had been at the outer periphery of the panels. The aluminum panels, having been extended toward the center of the antenna, were forced into a tighter bend at the inner edges. Once forced into furled position, the antenna would not deploy itself, even in the one-*g* field. The panels were tightly held by the subdish supports. Pulled past this binding point, considerable strain energy was released and, without holding the ribs as they opened, the assembly almost certainly would have been damaged.

After redeployment it was found that the inner portions of the panels had plastically deformed, and upward bumps were seen at the inner edges of each panel. An effort to relieve these by slitting along each hinge flange was unsuccessful. It was also found that, despite the small angles which had been incorporated into the hinges, the

aluminum panels were overpowering the ribs, producing a generally upward bend. Some thought was given to perforating the panels to weaken them and, at the same time, reduce weight. It was decided that too many other problems existed, and that a new design approach would be needed.

5. New Design

Experience with the thick, self-supporting membrane concept had not been promising. While early work with the 0.005-in.-thick stainless steel membrane had indicated it might work in zero g, testing in earth environment is highly desirable. Several concepts, including membranes intermediate in thickness to those already tried, and incorporating various stiffening members, were considered and rejected as too complex. However, the chances of success appeared good if a furlable outer ring could be provided, supported from the center hub by a minimum of radial ribs. Now, a compliant membrane made of strips to eliminate circumferential loads could be used as the reflector surface. The strips would be stretched between the center hub and the outer support ring. Experimentation with small models showed such a design concept is feasible. In this new design, the outer ring has a channel cross section, and is supported from the center hub by three radial ribs located 120 deg apart. In furling, the ribs raise to a vertical position, and the portions of the channel between the ribs loop downward. The channel legs are "hinged" at each corner of the channel section, to permit this deformation without plastic yielding. For the membrane reflector surface, aluminized Kapton was considered. It has better resistance to ultraviolet radiation than Mylar, but for the first experiment Mylar was chosen since it was readily available. A preliminary test series on ¼-, ½-, and 1-mil Mylar films showed that 5-gram/cm loading was adequate to stretch the material. It was decided that the ½-mil material showed most promise for the first antenna construction. Tensile tests of 2.5-cm-wide samples showed no tendency to develop wrinkles when stressed an order of magnitude over the 5-gram/cm loading. A sample was loaded unidirectionally to 15 grams/cm, and clamped in an aluminum frame 38×7.6 cm with the stress in the long direction. The assembly was immersed in liquid nitrogen to see if the material would stretch or rupture. It did not, and there was no change in apparent condition upon return to room temperature. Design of the new antenna has been completed and construction of a prototype is expected to begin shortly.